THE MEXICAN HAT WAVELET FAMILY. APPLICATION TO THE STUDY OF NON-GAUSSIANITY IN COSMIC MICROWAVE BACKGROUND MAPS

F. Argüeso[1], *J. L. Sanz*[2], *R.B. Barreiro*[2,3], *D. Herranz*[2], *J. González-Nuevo*[4]

[1]Departamento de Matemáticas, Universidad de Oviedo, 33007, Oviedo, Spain
email: argueso@uniovi.es
[2]Instituto de Física de Cantabria, 39005, Santander, Spain
[3]Departamento de Física, Universidad de Cantabria, 39005, Santander, Spain
[4]SISSA-I.S.A.S, via Beirut 4, I-34014,Trieste, Italy

ABSTRACT

The detection of the non-Gaussian signal due to extragalactic point sources and its separation from the possible intrinsic non-Gaussianity is an issue of great importance in the cosmic microwave background (CMB) analysis. The Mexican Hat Wavelet Family (MHWF), which has been proved very useful for the detection of extragalactic point sources, is applied here to the study of non-Gaussianity due to point sources in CMB maps. We carry out simulations of CMB maps with the characteristics of the forthcoming Planck mission at 70 and 100 GHz and filter them with the MHWF. By comparing the skewness and kurtosis of simulated maps with and without point sources, we are able to detect clearly the non Gaussian signal due to point sources for flux cuts as low as 0.4 Jy (70 GHz) and 0.3 Jy (100 GHz). The MHWF performs better in this respect than the Mexican Hat Wavelet and much better than the Daubechies 4 wavelet.

1. INTRODUCTION

According to the standard cosmological model, CMB temperature anisotropies are caused by the inhomogeneities in the distribution of matter and radiation present at the decoupling time, the time when the hydrogen atoms were formed from protons and electrons and the photons started to propagate freely, being observed now as the CMB. These inhomogeneities are the product of quantum fluctuations amplified in an era of exponential expansion at the beginning of the Universe, the inflationary era, and have an essentially Gaussian statistical distribution. Nevertheless, small non-Gaussianity can be introduced, for instance, by second order relativistic effects or by features in the scalar field potential which drives inflation [1]. The analysis of the first year Wilkinson Microwave Anisotropy Probe (WMAP) data show that temperature fluctuations of the CMB follow a Gaussian distribution [2] in agreement with the standard inflation paradigm. However, some studies have detected non-Gaussian features in the WMAP data, for instance in [3, 4] a cold non-Gaussian spot of unknown origin was detected by using the Mexican Hat Wavelet. On the other hand, astrophysical foregrounds contaminate the cosmological signal and give also rise to a non Gaussian contribution. In particular, the emission due to point sources (radio and infrared galaxies are seen as point-like objects due to their very small projected angular size as compared to the typical experimental resolutions) is clearly non Gaussian.

It is very important to assess the degree of non-Gaussianity generated by point sources in order to distinguish it from the non Gaussian signal coming from other origins. The ESA Planck satellite [5, 6], which will be launched in 2008, will analyze the CMB anisotropies with unprecedented accuracy and resolution and will make possible a very precise non-Gaussianity study, for which the use of wavelets can be very suitable.

The Mexican Hat Wavelet (MHW) has been very useful to detect point sources [7, 8] in CMB maps, by using the signal amplification going from real space to wavelet space. The Mexican Hat Wavelet Family (MHWF) was introduced in [9] as an extension of the standard MHW, which produced higher amplification and then a better performance at point source detection. The MHWF is a family of isotropic 2D wavelets obtained by applying the Laplacian operator iteratively to the 2D Gaussian.

The expression of these new wavelets in real space is

$$\psi_n(x) = \frac{(-1)^n}{2^n n!} \triangle^n \varphi(x) \tag{1}$$

where φ is the 2D Gaussian and $x = |\vec{x}|$.

$$\varphi(x) = \frac{e^{-x^2/2}}{2\pi} \tag{2}$$

Note that $\psi_1(x)$ is the standard MHW, we call the other corresponding members of the family MHWn. Any member of the family can be written very easily in Fourier space as

$$\hat{\psi}_n(k) = \frac{k^{2n} e^{-\frac{k^2}{2}}}{2^n n!} \tag{3}$$

In [9] we considered a point source convolved with a Gaussian beam (antenna) of dispersion γ and embedded in a CMB map. Then, we filtered the map with the first members of the MHWF at different scales R. The amplification, λ, is defined as the ratio between the intensity of the point source I_w and the rms deviation σ_w in the wavelet filtered image divided by this ratio in the original image filtered with a Gaussian-shaped beam.

$$\lambda = \frac{I_w/\sigma_w}{I_g/\sigma_g} \tag{4}$$

I_w can be calculated for the different members of the MHWF as [9]

$$I_w = \frac{I_g \beta^{2n}}{(1+\beta^2)^{n+1}} \quad (5)$$

with $\beta = R/\gamma$. It was proved in [9] that when filtering CMB maps with the first three members of the MHWF at an optimal scale, R, MHW2 and MHW3 produced a higher amplification than the standard MHW and were hence more effective at source detection. For n higher than 3 the amplification is not so high.

The detection of the non Gaussian signal due to point sources poses a similar problem, these new wavelets will enhance the signal (non Gaussian) due to point sources, making possible a more effective detection of this kind of non-Gaussianity. Since the skewness and kurtosis of a Gaussian distribution are zero and three respectively, any significant deviation from these values will mean the presence of a non Gaussian signal, so that the skewness and the kurtosis of the wavelet filtered maps can be used as estimators of the non-Gaussianity due to point sources.

The plan of the paper is as follows: In §2, we calculate the cumulants of a wavelet filtered map from those of the original map, this allows us to relate the skewness and kurtosis of the filtered maps with the amplification. In §3, we carry out realistic CMB simulations with and without point sources, considering the characteristics of the Planck experiment at 70 and 100 GHz and perform the non-Gaussianity detection by filtering with the MHWF. Finally in §4, we draw the main conclusions of the paper.

2. SKEWNESS AND KURTOSIS OF A WAVELET FILTERED MAP

Skewness and kurtosis provide us with suitable tests for determining whether certain data come from a Gaussian distribution or not. The skewness, s, is defined as

$$s = \frac{\mu_3}{\sigma^3} \quad (6)$$

where μ_3 is the third central moment of the distribution and σ its rms deviation, the skewness is zero for a Gaussian distribution. The kurtosis, k, is the fourth central moment divided by the variance to the square

$$k = \frac{\mu_4}{\sigma^4} \quad (7)$$

and its value is 3 in the Gaussian case. We are interested now in calculating the skewness and kurtosis due to point sources in a wavelet filtered map from these quantities in the original observed map. We consider then a pixelized 2D image including CMB, Galactic foregrounds, instrumental noise and extragalactic point sources; these four components are independent and are added up to form the image; whereas the CMB and the noise are Gaussian-distributed, the other two are non Gaussian.

Skewness and kurtosis can be obtained from the cumulants of the probability distribution function (pdf), these cumulants can be calculated as derivatives of the cumulant function, the logarithm of the characteristic function, which is the Fourier transform of the pdf. The second order cumulant is the variance, the third order cumulant is the third central moment μ_3 and the fourth order cumulant is $\mu_4 - 3\sigma^4$. The advantage of using the cumulants is that when the data are independent the cumulant of the sum is the sum of the cumulants. So, the cumulant of any order of the sum of CMB, point sources and other foregrounds is the sum of the cumulants of the components.

In a typical CMB experiment, the image is filtered with a Gaussian shaped beam, this means that the map is convolved with a Gaussian function. This convolution changes the skewness and kurtosis of the original map. When we consider the point sources, the convolution implies that the temperature of a pixel is a linear combination of the temperatures of the neighboring pixels, which are not correlated. The cumulants of this linear combination can then be written as a linear combination of the cumulants. If we are filtering with a function $\varphi(\vec{x})$, the cumulant of order m, K_m^f, of the filtered image can be written as

$$K_m^f = K_m A_p^{m-1} \int \varphi^m(\vec{x})\, d\vec{x} \quad (8)$$

where K_m is the original cumulant of order m and A_p the pixel area. From this formula, we can obtain the cumulants of the Gaussian filtered image from those of the original one. Note that Eq.(8) is only valid if the data are uncorrelated, which is true for point sources and the instrumental noise but not for the CMB and Galactic foregrounds. However, since the CMB and the noise are considered as Gaussian, they do not produce a non Gaussian signal and the level of non Gaussianity due to Galactic foregrounds is negligible compared to that of point sources, at least for the frequencies analyzed in this work. This means that the main contribution will come from point sources, to which we can apply Eq.(8).

We are going to filter now the image with the first three members of the MHWF, the whole process amounts to filter the original image with a convolution of the Gaussian beam and the corresponding wavelets. We could then apply Eq.(8) with $\varphi(\vec{x})$ this convolution. Finally, we can relate the cumulants K_m^w of the wavelet filtered image to the cumulants K_m^g in the Gaussian filtered image, which is the observed one.

$$K_m^w = K_m^g \frac{m(2\pi)^m \beta^{2-2m} C_{mn}}{(1+\beta^{-2})^{(n+1)m-1}} \quad (9)$$

in this formula, n is the wavelet index and the coefficients C_{mn} are calculated as

$$C_{mn} = \int (\psi_n(x))^m x\, dx \quad (10)$$

This last expression can be easily computed for the first members of the MHWF and for m=3,4.

When we consider the skewness of the total wavelet filtered image (CMB+point sources+Galactic foregrounds+noise), it can be obtained as the total third order cumulant divided by σ_w^3 with σ_w the total rms deviation. The contribution of point sources to the total skewness of the wavelet filtered map is

$$\hat{s}_w = \frac{K_3^w}{\sigma_w^3} \quad (11)$$

where K_3^w is the third order cumulant (due to point sources) of the wavelet filtered map. The contribution of point sources to the total skewness of the Gaussian filtered map is

$$\hat{s}_g = \frac{K_3^g}{\sigma_g^3} \quad (12)$$

where K_3^g is the third order cumulant (due to point sources) of the Gaussian filtered map and σ_g the total rms deviation of the Gaussian filtered maps. Finally we can relate $\hat{s}_w$ and $\hat{s}_g$ by using eqs.(4),(5) and (9). We obtain the following formula for the MHW

$$\hat{s}_w = \frac{4}{9}(1+\beta^2)\lambda^3\hat{s}_g \tag{13}$$

For the MHW2, we obtain a similar formula

$$\hat{s}_w = \frac{22}{81}(1+\beta^2)\lambda^3\hat{s}_g \tag{14}$$

and finally for the MHW3

$$\hat{s}_w = \frac{1240}{6561}(1+\beta^2)\lambda^3\hat{s}_g \tag{15}$$

We want to point out that these contributions depend on the amplification to the cube and will be higher for the wavelets with the highest amplifications, this suggests that MHW2 and MHW3 can be better at detecting non-Gaussianity due to point sources than MHW. Besides, we will choose optimal scales when filtering with the MHWF so that the contribution to the skewness is maximum. The optimal scales can be determined by using simulations (see next section).

We can also obtain similar relations between the contribution of point sources $\hat{k}_w$ to the kurtosis of the wavelet filtered maps and the contribution of point sources $\hat{k}_g$ to the kurtosis of the beam filtered maps. So, we have for the MHW

$$(\hat{k}_w - 3) = \frac{15}{32}(1+\beta^2)\lambda^4(\hat{k}_g - 3) \tag{16}$$

for the MHW2

$$(\hat{k}_w - 3) = \frac{2547}{8192}(1+\beta^2)\lambda^4(\hat{k}_g - 3) \tag{17}$$

and for the MHW3

$$(\hat{k}_w - 3) = \frac{61731}{262144}(1+\beta^2)\lambda^4(\hat{k}_g - 3) \tag{18}$$

In this case, the contribution of point sources to the total kurtosis in the wavelet filtered map is proportional to λ^4.

3. NON-GAUSSIANITY OF SIMULATED CMB MAPS

In this section, we are going to consider the study of the non-Gaussianity in realistic simulated CMB maps. We have carried out simulations of CMB 2D maps of 12.8×12.8 square degrees, generated with the cosmological parameters of the standard model. We have then added the relevant Galactic foregrounds (free-free, synchrotron and dust emission), we have used the Planck Reference Sky, prepared by the members of the Planck Working Group 2 and available at www.planck.fr/heading79.html.

In order to give the most realistic numbers of detected extragalactic point sources, we have adopted the model recently presented by [10]. This new model has proven capable of giving a better fit than before to all the currently published source number counts and related statistics at $\nu \geq 10$ GHz coming from different surveys [11, 12].

Since we are specially interested in applying our new method to the maps which will be provided by the *Planck* mission in the next future, and given that we can be very confident in the input source model counts, we have considered the specific conditions of two *Planck* channels, which operate at 70 and 100 GHz.[1]

We consider 1000 simulations of CMB plus noise at 70 and 100 GHz, these simulations are Gaussian and will serve us to compare them with the non-Gaussian ones. We filter these simulations with the MHW, MHW2 and MHW3 at the optimal scales (those which produce the highest amplification) and calculate their skewness and kurtosis. Then, we generate 1000 simulations including CMB, noise, Galactic foregrounds and point sources for each of the following flux cuts: 1Jy, 0.9 Jy, 0.8 Jy,.....,0.1 Jy, we assume that this is the flux above which we have removed all the sources. We filter these simulations as before with the first members of the MHWF at the optimal scales, obtained by maximizing the amplification.

Now, taking into account the skewness, we perform the following hypothesis test: we consider the null hypothesis, H_0, the simulation is Gaussian, against the alternative hypothesis, H_1, it is non Gaussian. We set a significance level $\alpha = 0.05$, this means that we reject the null hypothesis when a simulation with point sources has a skewness higher than that of 95% of the Gaussian simulations. The test is one-sided to the right, since the simulations with point sources have positive skewness. We define the power of the test as $1-\delta$, with δ the probability of accepting the null hypothesis when it is false, i.e. the power is the proportion of non-Gaussian simulations with a skewness higher than that of 95% of the Gaussian ones. The higher the power, the more efficient the method at detecting non-Gaussianity.

We perform the same test with the kurtosis; it is also one-sided to the right, since the kurtosis of point sources is higher than 3.

In Figure 1, we plot the power of the skewness test at 70 GHz against the flux cut for the MHW, MHW2 and MHW3; it is clear that the MHW2 and MHW3 have higher power than the MHW. Logically, the power increases with the flux cut, but the power is as high as 22% for the MHW, 30% for the MHW2 and 26% for the MHW3 at 0.6 Jy. We have plotted the power of the kurtosis test in Figure 2, in this case the power is higher: 35% for the MHW, 42% for the MHW2 and 42% for the MHW3 at 0.6 Jy. The number of simulations (1000) seems enough in order to get stable powers. In a real experiment we could study at least half the sky (126 simulations of the size we have considered), so that by using real data with this flux cut, the detection of non-Gaussianity would be clear. The power for the kurtosis test (MHW2) is 28% at 0.5 Jy and 18% at 0.4 Jy, in these cases we could also detect the non-Gaussianity due to point sources.

We have performed the same tests for the 100 GHz channel, the results are plotted in Figures 3 (skewness) and 4 (kurtosis); now the power is higher than for the 70 GHz channel. For instance, at 0.6 Jy the power (skewness) is 59% (MHW), 74% (MHW2) and 76% (MHW3), whereas the power of

[1] The characteristics of the channels, relevant for our purposes, are: a) pixel sizes, $3'$ and $3'$ at 70 and 100 GHz, respectively; b) Full Width Half Maximum (FWHM) of the circular gaussian beams, $14'$ and $9.5'$, respectively; c) thermal (uniform) noises, in units of $\Delta T/T$ per pixel, with T the thermodinamic temperature, $\sigma = 4.7 \times 10^{-6}$ and $\sigma = 2.5 \times 10^{-6}$, respectively, in a square whose side is the FWHM extent of the beam. In all the cases, we have used the estimated instrument performance goals available at the web site: $http://astro.estec.esa.nl/Planck$.

the kurtosis test is 82% (MHW), 90% (MHW2) and 92% (MHW3). The power of the kurtosis test at 0.3 Jy is 44% (MHW2) and 46% (MHW3). In this case, the non Gaussian signal would be clearly detected till this flux, when we go down to lower fluxes the power decreases very quickly (see Figure 4).

In order to assess the influence of the Galactic foregrounds, we have also carried out 1000 simulations without point sources but including the Galactic foregrounds. The power in this case is always below 10%, confirming a very small contribution of these foregrounds to the non-Gaussianity.

We have also performed similar tests by filtering the maps with the Daubechies 4 wavelet, this wavelet has been already used in the study of the non-Gaussianity of CMB maps [13]. The power of the skewness and kurtosis tests with this wavelet is never higher than 20%, even for fluxes as high as 1 Jy. We have considered skewness and kurtosis of different detail coefficients (horizontal, vertical, diagonal) at different resolution levels. It is clear that whereas the members of the MHWF are adapted to the detection of point sources and the non Gaussian signal they produce, this is not the case for the Daubechies family.

4. CONCLUSIONS

We have considered a natural generalization of the MHW on the plane, R^2, based on the iterative application of the Laplacian operator to the MHW. We have called this group of wavelets the Mexican Hat Wavelet Family (MHWF) [9]. We have applied the MHWF to the study of the non-Gaussianity produced in CMB maps by extragalactic point sources, a very important issue for the separation and analysis of different non Gaussian components in the CMB.

We have first derived a series of formulas, equations (13-18), which relate the contribution of point sources to the skewness and kurtosis of wavelet (MHWF) filtered 2D CMB maps with their contribution to the skewness and kurtosis of beam filtered CMB maps. According to these formulas, the skewness of a wavelet filtered map is proportional to λ^3, with λ the amplification and the kurtosis is proportional to λ^4. This means that the higher the amplification the higher will be the non Gaussian signal, this effect is dominant with respect to other factors in eqs. (13-18) . So, the MHW2 and MHW3 at their optimal scales can be very suitable filters to detect the non Gaussian signal due to point sources, since they produce a higher amplification than the MHW [9]; .

We have then considered Gaussian simulations of CMB plus noise and compared them with simulations including all the relevant components: CMB, noise, point sources and Galactic foregrounds. The simulations are 2D maps of 12.8×12.8 square degrees with the characteristics of the Planck experiment at 70 GHz and 100 GHz. We perform a Gaussianity test based on the skewness and kurtosis of the maps filtered with the MHW, MHW2 and MHW3 at the optimal scales; we compare 1000 simulations of CMB plus noise with 1000 simulations including point sources till different flux cuts. We are able to detect clearly the non Gaussian signal due to point sources for flux cuts as low as 0.4 Jy (70 GHz) and 0.3 Jy (100 GHz)

MHW2 and MHW3 perform better than MHW at detecting non-Gaussianity produced by point sources. The kurtosis test is more powerful than the skewness one and the power is higher at 100 GHz than at 70 GHz.

This method could be used for all the frequencies of the Planck experiment and could also be extended to spherical CMB images, as the ones provided by the Planck experiment.

Acknowledgments

We acknowledge partial financial support from the Spanish Ministry of Education (MEC) under project ESP2004–07067–C03–01. DH acknowledges a Juan de la Cierva contract of the MEC. We thank G. De Zotti for having kindly provided us with the source number counts foreseen by the De Zotti et al. (2005) cosmological evolution model at the LFI frequencies. We acknowledge the use of the Planck Reference Sky, prepared by the members of the Planck Working Group 2, and available at www.planck.fr/heading79.html. We also thank L. Toffolatti for useful discussions.

REFERENCES

[1] Bartolo, N. et al. " Non Gaussianity from inflation: theory and observations", 2004, Phys. Rept., 402, 103

[2] Komatsu, E. et al. "First Year Wilkinson Microwave Anisotropy Probe (WMAP) Observations: Tests of Gaussianity ", 2003, ApJ Suppl.,148, 119

[3] Vielva, P. et al., "Detection of non-Gaussianity in the WMAP 1-year data using spherical wavelets", 2004, ApJ, 609, 22

[4] Cruz, M. et al., " Detection of a non-Gaussian Spot in WMAP", 2005, MNRAS, 356, 29

[5] Mandolesi, N. et al., 1998, Proposal for the "Planck" Low Frequency Instrument (LFI), ESA Science Report D(SCI)-98(03)

[6] Puget, J. L. et al. 1998, Proposal for the "Planck" High Frequency Instrument (HFI), ESA Science Report D(SCI)-98(03)

[7] Cayón, L. et al. "Isotropic Wavelets: a Powerful Tool to Extract Point Sources from CMB Maps", 2000, MNRAS, 313, 757

[8] Vielva, P. et al. "Point Source Detection using the Spherical Mexican Hat Wavelet on simulated all-sky Planck maps", 2003, MNRAS, 344, 89

[9] Argüeso, F. et al.," The Mexican Hat Wavelet Family. Application to point source detection in cosmic microwave background maps", 2005, Proceedings of the 13th European Signal Processing Conference " EUSIPCO 2005 ", Antalya (Turkey).

[10] De Zotti, G. et al., "Predictions for high-frequency radio surveys of extragalactic sources ", 2005, A&A, 431, 893

[11] Waldram, E. et al."9C: A Survey of Radio Sources at 15 GHz with the Ryle Telescope", 2003, MNRAS, 342, 915

[12] Ricci, R. et al. "First results from the ATCA 18 GHz pilot survey" ,2004, MNRAS, 354, 305

[13] Barreiro, R. B., Hobson, M. P. " The discriminating power of wavelets to detect non-Gaussianity in the CMB ", 2001, MNRAS, 327, 813

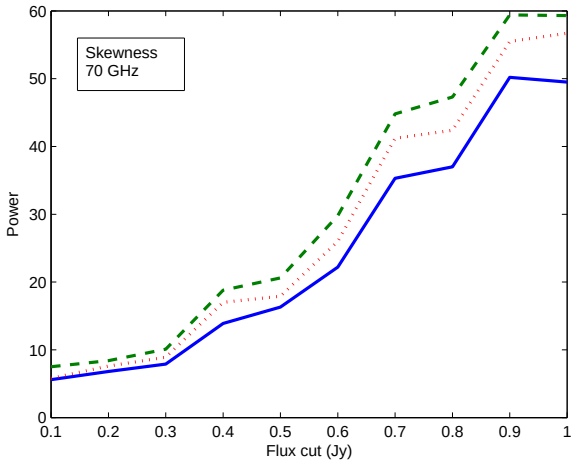

Figure 1: power of the skewness test at 70 GHz against the flux cut for the MHW (solid line), MHW2 (dashed line) and the MHW3 (dotted line).

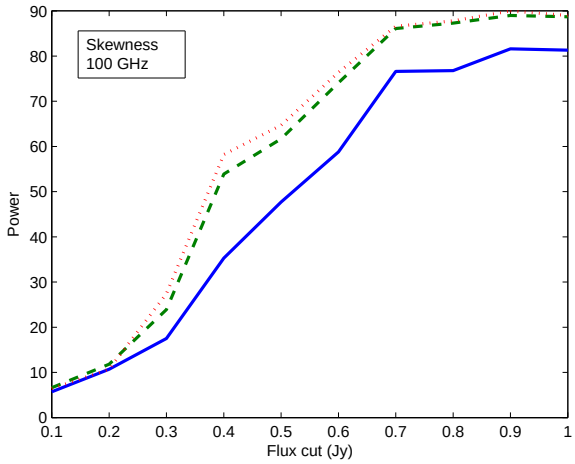

Figure 3: power of the skewness test at 100 GHz against the flux cut for the MHW (solid line), MHW2 (dashed line) and the MHW3 (dotted line).

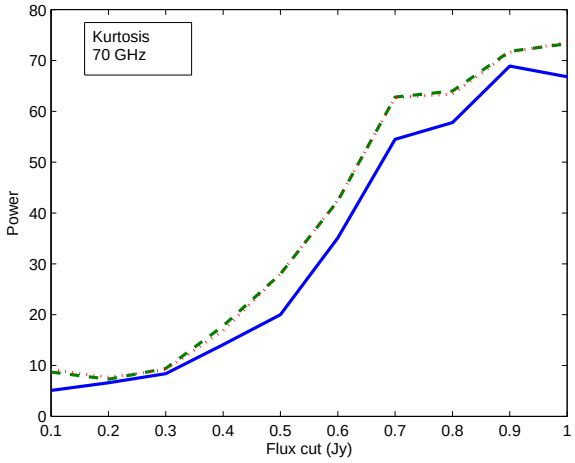

Figure 2: power of the kurtosis test at 70 GHz against the flux cut for the MHW (solid line), MHW2 (dashed line) and the MHW3 (dotted line).

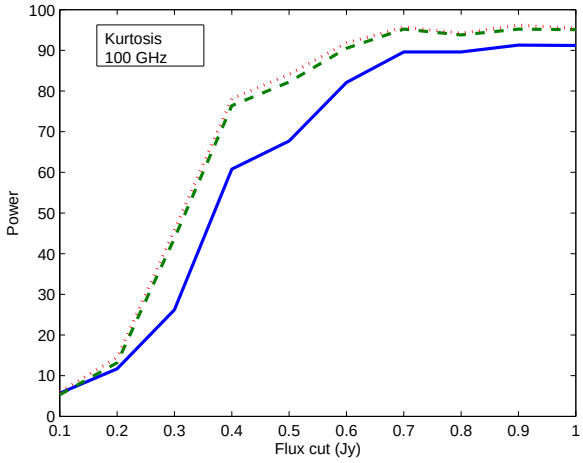

Figure 4: power of the kurtosis test at 100 GHz against the flux cut for the MHW (solid line), MHW2 (dashed line) and the MHW3 (dotted line).